Ultrastructural and functional alterations of mitochondria in perilesional vitiligo skin

Francesca Prignano [a,*], Leonardo Pescitelli [a], Matteo Becatti [b], Paola Di Gennaro [a], Claudia Fiorillo [b], Niccolò Taddei [b], Torello Lotti [a]

[a] Department of Dermatological Sciences, University of Florence, Florence, Italy
[b] Department of Biochemical Sciences, University of Florence, Florence, Italy

ARTICLE INFO

ABSTRACT

Background: Vitiligo is a chronic acquired hypomelanotic disorder affecting 0.5–2% of the world's population. The two major pathogenetic hypotheses are focused on immune-mediated or toxic-mediated cell damage primarily directed at melanocytes. Recent experimental data underline the complex interactions that exist between melanocytes and other cells found in the skin.
Objective: Among these cells, keratinocytes are able to influence both the survival and the functional activity of melanocytes. In order to gain insights into the involvement of different types of epidermic cells in the pathogenesis of vitiligo, we have performed an ultrastructural study on lesional, perilesional and normal skin from 12 patients. All these patients suffered from non-segmental vitiligo, with a similar clinical history in terms of lesion extension and duration of the disease.
Methods: We have therefore grown cultures of keratinocytes from lesional, perilesional and healthy skin, evaluating the presence of oxidative damage and apoptotic markers in the cells.
Results: Taken together, our results indicate that keratinocytes from perilesional skin show features of damaged cells.
Conclusion: Our data, besides considering the achromic patch as the terminal event of a chain of biological processes that take place in the perilesional skin, highlight keratinocytes as having an important role in the development of vitiligo.
© 2009 Japanese Society for Investigative Dermatology. Published by Elsevier Ireland Ltd. All rights reserved.

1. Introduction

Vitiligo is a chronic acquired hypomelanotic disorder affecting 0.5–2% of the world's population, without any racial, sexual or regional differences in prevalence [1,2].

This disease is characterised by the loss of melanocytes in the epidermis (and probably in other organs). The selective destruction of skin melanocytes results in the development of white patches often surrounded by hyperpigmented skin. These patches, which are initially small, progressively increase in size and tend to form larger patches. These patches can break out in virtually any part of the body although the face, the back of the hands, wrists, axillae, umbilicus and genitalia are the regions that are most often affected [3,4].

Several types of vitiligo have been described, according to the distribution of the achromic lesions. One or more lesions in a dermatomal pattern are characteristic of segmental vitiligo while this segmental distribution is absent in focal vitiligo. Both are localised types of vitiligo. Generalized vitiligo is characterised by the symmetrical distribution of multiple scattered lesions [5,6].

In contrast to the ease of clinical diagnosis, the cellular mechanisms and biochemical changes leading to the appearance of the achromic lesions are still uncertain.

There are three major pathogenetic hypotheses. The auto-immune theory proposes that melanocytes are killed by an immune-mediated mechanism, involving either cytotoxic memory T cells or autoantibodies directed against melanocyte-surface antigens, as a result of a breakdown in tolerance [7]. This hypothesis is supported by the frequent association of vitiligo with autoimmune diseases, such as autoimmune thyroiditis, diabetes mellitus, pernicious anemia and alopecia areata, and by the effectiveness of immunomodulatory agents, such as corticosteroids and calcineurin inhibitors, in the treatment of vitiligo [8].

The biochemical hypothesis states that the autocytotoxic metabolites of melanin synthesis are responsible for the destruction of melanocytes [9]. Furthermore, several studies suggest that the possible damage brought about by increased intracellular oxidative stress would lead to the functional impairment of

* Corresponding author.
E-mail address: francesca.prignano@unifi.it (F. Prignano).

melanocytes [10]. Increased levels of pro-oxidants, as well as decreased levels of anti-oxidant agents, have been found in the blood of patients suffering from vitiligo [11]. Moreover, other studies indicate the presence of oxidative stress-induced damage within the epidermis of vitiliginous lesions [12].

Segmental vitiligo is best explained by the neural theory. According to this hypothesis, some chemical mediators released from peripheral nerve endings cause decreased melanin production [13,14].

Patients affected by vitiligo show an enhanced production of GTP-cyclohydrolase I leading to an excessive de novo synthesis of (6R)5,6,7,8 tetrahydrobiopterin (6-BH-4). Continuous production of 6-BH-4 leads to increased synthesis of the catecholamines in keratinocytes, leading to an excess of norepinephrine in both the plasma and urine of these patients [15,16]. In addition to a direct cytotoxic effect, catecholamine metabolites could exert an indirect action through the activation of the α-adrenergic receptors of skin arterioles, eventually leading to vasoconstriction. Severe or repeated attacks of hypoxia cause toxic oxygen radicals to accumulate, resulting in depigmentation [17]. Recent studies have reported ultrastructural evidence of axonal damage in the nerves of segmental vitiliginous lesions, which supports this hypothesis [18].

According to all these pathogenetic mechanisms, vitiligo can be viewed as an event that only affects, whether primarily or secondarily, melanocytic cells. None of them takes into account the interactions of melanocytes with other epidermal or dermal cells, which are able to influence both the functional activity and the survival of melanocytes. Recent experimental data underlines the complex interactions that exist between melanocytes and other cutaneous cells, such as keratinocytes, Langerhans cells, endothelial cells, fibroblasts and mast cells [19–23].

This data supports the concept of the epidermal melanic unit proposed by Fitzpatrick and Breathnach [24], as it highlights the central role that melanocytes play in receiving the stimulating and/or inhibitory signals produced by keratinocytes, mast cells, fibroblasts, lymphocytes, macrophages, and nerve endings. An alteration of the microenvironment, which is composed of cytokines and growth factors, may lead to melanocyte dysfunction, as a result of its early apoptotic death. Therefore, vitiliginous achromic lesions may be the result of altered signaling, which is characterised by a dominant inhibiting effect. According to this relatively new etiopathogenetic mechanism – the so-called "eclectic hypothesis" [25] – vitiligo is the expression of a change in the normal communication network, involving melanocytes, keratinocytes, mast cells and fibroblasts,

which results in a biochemical imbalance (related to growth factors, cytokines, inflammatory mediators and adhesion molecules) that does not permit melanocytic survival in the epidermal environment. The creation of an adverse microenvironment would induce the early death of melanocytes by apoptosis and the formation of achromic lesions. These become permanent because healthy melanocytes and reservoir cells are unable to colonise such areas [26,27].

Previously published data on the ultrastructural features of lesional, perilesional and normal skin from patients that have vitiligo is conflicting. This is mainly due to the fact that skin samples are often collected at different stages in the course of the disease [28–32]. In order to clarify these discrepancies, we have performed an ultrastructural study of lesional, perilesional and normal skin from 12 patients with non-segmental vitiligo, all of which had a similar clinical history with respect to lesion extension and duration of the disease. In our study, lesional, perilesional and healthy skin is defined as clinically affected skin (lesional), skin along the edge of the white patch (perilesional) and clinically unaffected, normally pigmented skin (healthy). We have therefore grown keratinocytes cultures from lesional, perilesional and healthy skin to evaluate the presence of oxidative damage and apoptotic markers in the cells.

2. Materials and methods

Punch-biopsies of 6 mm were taken from lesional, perilesional and healthy skin of 12 patients affected by non-segmental vitiligo. The clinical information of each patient is summarised in Table 1. Written permission was obtained from all patients. Procedures were carried out in accordance with the ethical standards of the Committees on Human Experimentation of the Dipartimento di Scienze Morfologiche. The study was conducted in accordance with the Declaration of Helsinki.

2.1. Keratinocyte isolation and culture

Each single biopsy (from lesional, perilesional and healthy skin) from each patient was cut into two pieces: one half was prepared for cell culture and the other half – which was further divided into two – for conventional microscopy and for electron microscopy.

2.2. Cell culture

The fat and the subcutis was removed from the small skin specimen (from lesional, perilesional and healthy skin of each

Table 1
Clinical data of vitiligo patients.

Patients	Age	Clinical type of vitiligo	Age of onset	Biopsy site (lesional and perilesional skin)[a]	Biopsy site (healthy skin)[a]
M[b]1	43	NS[c] generalized	19	Trunk	Abdomen
M2	51	NS generalized	6	Trunk	Abdomen
M3	47	NS generalized	11	Abdomen	Trunk
M4	39	NS generalized	5	Pubis	Abdomen
M5	52	NS generalized	25	Abdomen	Trunk
M6	45	NS localised	21	Trunk	Abdomen
F[d]1	44	NS generalized	31	Abdomen	Trunk
F2	38	NS generalized	20	Trunk	Abdomen
F3	49	NS generalized	13	Trunk	Abdomen
F4	42	NS generalized	33	Pubis	Abdomen
F5	50	NS generalized	27	Abdomen	Trunk
F6	46	NS localised	18	Trunk	Abdomen

[a] Vitiligo was considered to be stable, as no new lesions or enlargement of old lesions occurred in the last 3 years.
[b] Male.
[c] Non-segmental vitiligo.
[d] Female.

patient) through the use of surgical scissors and washed several times in a buffered saline solution (PBS), to which antibiotics and antimycotics were also added. Each piece was further cut into many tiny pieces. The first enzymatic digestion was performed with collagenase (Sigma, Milan, Italy), for 3 h at 37 °C in a 5% CO_2 humidified atmosphere, in RPMI 1640 medium with 1% penicillin/streptomycin (Sigma–Adrich, Milan, Italy). The medium containing the cells was then centrifuged and the supernatant was discarded. A second enzymatic digestion was then performed with Trypsin/EDTA for 2 h at 37 °C in a 5% CO_2 humidified atmosphere. The enzymatic digestion was stopped using a Trypsin Neutralising Solution (Cambrex, Italy) and EDTA. The cells were then washed three times and finally put in KGM-2 BulletKit (Cambrex, Italy) until they reached confluence. When the cells reached confluence, they were cut and, after an internal immunostaining control with pancytokeratin-antibody (Sigma, Milan, Italy), further cultivated for many consecutive passages in KGM-2 BulletKit.

2.3. Immunofluorescence

The expression of cytokeratines was evaluated at each passage in vitro by a positive staining to pan-cytokeratin-antibody (Fig. 1) in order to assess the maintenance of the same immunophenotype. At the first passage, the absence of vimentin expression induced us to exclude the presence of any fibroblasts.

2.4. Electron microscopy

A quarter of each skin biopsy (of lesional, perilesional and healthy skin) was fixed in a mixture of 2% formaldehyde and 2.5% gluteraldehyde in 0.1 mmol/l cacodylate buffer, pH 7.4, at 5 °C for 3 h, followed by postfixation in 1% OsO_4 in phosphate buffer, pH 7.4, at room temperature for 2 h. The specimens were dehydrated in a graded acetone series, passed through propylene-oxide and embedded in epon 812. A sequential number of semithin sections were coloured with toluidine blue, while ultrathin sections were stained with uranyl acetate, followed by bismuth subnitrate or lead citrate, and examined in a Jeol 1010 (Tokyo, Japan) at 80 kV.

2.5. Preparation of cell homogenates

Keratinocytes (1×10^6) were washed twice with phosphate buffer saline (PBS), trypsinised, centrifuged and then resuspended
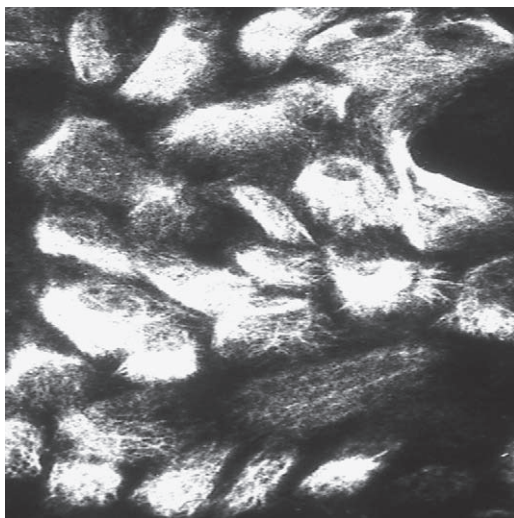

Fig. 1. Direct immunofluorescence: keratinocytes showing a clear-cut positivity for pan-anti-cytokeratin antibody. Third passage in vitro (150×).

in 100 μL of Lysis buffer containing 1% Triton X-100, 20 mM Tris–HCl pH8, 137 mM NaCl, 10% (v/v) Glycerol, 2 mM EDTA and 6 M urea supplemented with 0.2 mM PMSF, as well as 10 μg/ml leupeptin and aprotinin. To obtain cell homogenates, samples, after three freeze–thaw cycles, were twice sonicated in ice for 5 s and then centrifuged at $14,000 \times g$ for 10 min at 4 °C. The supernatant was then collected. The protein concentration was determined according to the Bradford method [33].

2.6. Determination of intracellular ROS

Cells were cultured on glass coverslips and loaded with dye by adding the ROS-sensitive fluorescent probe CM-H_2, DCFDA, dissolved in 0.1% DMSO (2.5 μM) and pluronic acid F-127 (0.01%, w/v), to the cell culture media for 10 min at 37 °C. The cells were fixed in 2.0% buffered paraformaldehyde for 10 min at room temperature and the DCF fluorescence analysed (at an excitation wavelength of 488 nm) using a confocal Leica TCS SP5 scanning microscope (Mannheim, Germany) equipped with an argon laser source for fluorescence measurements. The observations were performed by collecting the emitted fluorescence with a Leica Plan Apo 63x oil immersion objective. A series of 1.0 μm-thick optical sections (1024 × 1024 pixels) of the cells was taken at intervals of 0.5 μm. A number of optical sections (ranging from 10 to 20) for each examined sample were then projected as a single composite image by superimposition.

Reactive oxygen species (ROS) generation was also monitored by flow cytometry. Single-cell suspensions of cells were incubated with DCFH-DA (1 μM) at 37 °C for 15 min and immediately analysed by flow cytometry.

2.7. Total antioxidant capacity (TAC)

Intracellular TAC, accounting for total hydrophilic ROS scavengers, was measured in cell lysates by a chemiluminescence assay using the photoprotein Pholasin (Abel Antioxidant Test Kit, Knight Scientific Limited, UK). After washing with PBS, cells were resuspended in 20 mM Tris–HCl buffer, pH 8.0, containing 1.0% Triton, 137 mM NaCl, 10% glycerol, 6.0 M urea, 0.1 mM PMSF, 10 μg/ml leupeptin and 10 μg/ml aprotinin prior to storage at −80 °C until use. Cell plasma membranes were broken by three freeze-thaw cycles, 5.0 s sonication in ice and centrifugation at $14,000 \times g$ for 10 min at 4.0 °C. Protein content in the soluble fraction was measured by the method of Bradford. The results were calculated using an L-ascorbic acid-based standard curve.

2.8. Evaluation of lipid peroxidation

To assess the rate of lipid peroxidation, isoprostane levels were measured in cell lysates using the 8-isoprostane EIA kit (Cayman Chemical Company, Ann Arbor, MI, USA), following the manufacturer's instructions. Lipid peroxidation was also investigated by confocal scanning microscopy using BODIPY, a fluorescent probe that is intrinsically lipophilic and thus mimics the properties of natural lipids [34]. BODIPY 581/591 C_{11} acts as a fluorescent lipid peroxidation reporter that shifts its fluorescence from red to green in the presence of oxidising agents. Briefly, cells were cultured on glass coverslips and loaded with dye by adding the fluorescent probe BODIPY, dissolved in 0.1% DMSO (5 μM final concentration), to the cell culture media for 30 min at 37 °C. The cells were fixed in 2.0% buffered paraformaldehyde for 10 min at room temperature and the BODIPY fluorescence analysed (at an excitation wavelength of 581 nm) using a confocal Leica TCS SP5 scanning microscope (Mannheim, Germany) equipped with an argon laser source for fluorescence measurements. The observations were

performed by collecting the emitted fluorescence with a Leica Plan Apo 63x oil immersion objective. A series of 1.0 μm-thick optical sections (1024 × 1024 pixels) of the cells was taken at intervals of 0.5 μm. A number of optical sections (ranging from 10 to 20) for each examined sample were then projected as a single composite image by superimposition.

Lipid peroxidation was also quantified by flow cytometry. Single-cell suspensions were washed twice with PBS and incubated, in the dark, for 30 min at 37 °C with BODIPY 581/591 (2 μM) in DMEM. After labelling, cells were washed and resuspended in PBS and analysed using a FACSCanto flow cytometer (Becton-Dickinson, San Jose, CA).

2.9. Mitochondrial activity assay

Mitochondrial activity was assessed by the 3-(4,5-dimethylthiazol-2-yl)-2,5-diphenyltetrazolium bromide (MTT) assay in a 96-well plate [35]. After washing with PBS, 100 μl of 0.5 mg/ml MTT solution in PBS was added to the cell cultures and the samples were incubated for 4.0 h at 37 °C. Finally, 100 μl of cell lysis buffer (20% SDS, 50% N,N-dimethylformamide, pH 4.7) was added to each well and the samples were incubated for at least 3 h at 37 °C in a humidified incubator, before absorbance values of blue formazan were determined at 590 nm using an ELISA plate reader. Cell viability was expressed as percent of MTT reduction.

2.10. Mitochondrial permeability

Mitochondrial permeability was measured by calcein fluorescence according to the method described by Petronilli et al. [36],

albeit with minor modifications. Briefly, calcein/AM freely enters the cell and emits fluorescence upon de-esterification. Co-loading of cells with cobalt chloride quenches the fluorescence in the cell except in mitochondria—this is because cobalt cannot cross mitochondrial membranes (living cells). During induction of the MPT, cobalt can enter the mitochondria and is able to quench calcein fluorescence (apoptotic cells). Thus, decreased mitochondrial calcein fluorescence can be taken as a measure of the extent of MPT induction. Cells were cultured on glass coverslips and loaded with dye by adding the fluorescent probes calcein-AM (3 μM) and cobalt chloride (1 mM) to the cell culture media for 20 min at 37 °C.

Following cobalt quenching, cells were washed with HBSS and fixed in 2.0% buffered paraformaldehyde for 10 min at room temperature and the fluorescence analysed (at excitation wavelengths of 488 and 543 nm) using a confocal Leica TCS SP5 scanning microscope (Mannheim, Germany) equipped with an argon laser source for fluorescence measurements. The observations were performed by collecting the emitted fluorescence with a Leica Plan Apo 63x oil immersion objective. A series of 1.0 μm-thick optical sections (1024 × 1024 pixels) of the cells was taken at intervals of 0.5 μm. A number of optical sections (ranging from 10 to 20) for each examined sample were then projected as a single composite image by superimposition.

Mitochondrial permeability was also quantified by flow cytometry. Briefly, single-cell suspensions were incubated with the fluorescent probes calcein-AM (3 μM) and cobalt chloride (1 mM) for 20 min at 37 °C, washed twice with PBS and analysed using a FACSCanto flow cytometer (Becton-Dickinson, San Jose, CA).
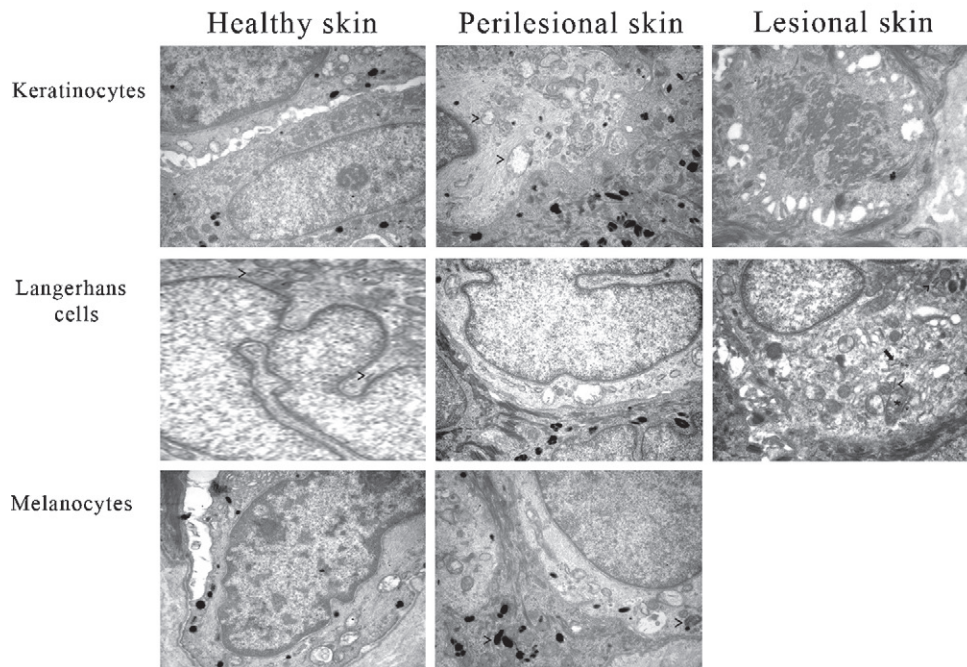

Fig. 2. A keratinocyte of healthy skin. An ultrastructural picture of a keratinocyte with no modification or alteration of the organelles (EM 12.000×). A keratinocyte of perilesional skin. Most of the mitochondria within the cell show an ultrastructural alteration: a swelling of their membranes (arrowhead) or a rearrangement of the cristae (EM 12.000×). A keratinocyte of lesional skin. The cell shows a rich cytoskeleton with no alterations of the organelles (EM 10.000×). A Langerhans cell of healthy skin. A typical dendritic cell with a polilobulated nucleous and some Birbeck granules within the cytoplasm (arrowhead) (EM 12.000×). A Langerhans cell of perilesional skin. The cell shows the characteristic intended nucleous and no organelles alterations: (EM 12.000×). A Langerhans cell of lesional skin. The cell shows many Birbeck granules within the cytoplasm; some with the characteristic racket-like shape (arrow) and some others without the terminal gemmation (arrowhead). A large mitochondria within the cytoplasm (asterisk): (EM 12.000×). A melanocyte of healthy skin. The cell shows addensed chromatin within the nucleous, a normal distribution of organelles and some melanosomes within the cytoplasm: (EM 12.000×). A melanocyte of perilesional skin. Many melanosomes are detectable within the cell at various degree of differentiation (arrowhead): (EM 12.000×).

2.11. Confocal microscope imaging of caspase activity

Cells were cultured on glass coverslips and the culture media removed and replaced with FAM-FLICA™ Caspases 3&7 solution (Caspase 3&7 FLICA kit FAM-DEVD-FMK), FAM-FLICA™ Caspases 8 solution (Caspase 8 FLICA kit FAM-LETD-FMK) and FAM-FLICA™ Caspases 9 solution (Caspase 9 FLICA kit FAM-LEHD-FMK), Immunochemistry Technologies, LLC, Bloomington, MN, for 1 h, following the manufacturer's instructions. Cells were washed three times with a wash buffer provided with the kit and fixed in 2.0% buffered paraformaldehyde for 10 min at room temperature. Fluorescence was detected at an excitation wavelength of 488 nm using a confocal Leica TCS SP5 scanning microscope (Mannheim, Germany) equipped with an argon laser source for fluorescence measurements. The observations were performed by collecting the emitted fluorescence with a Leica Plan Apo 63x oil immersion objective. A series of 1.0 μm-thick optical sections (1024 × 1024 pixels) of the cells was taken at intervals of 0.5 μm. A number of optical sections (ranging from 10 to 20) for each examined sample were then projected as a single composite image by superimposition.

2.12. Assessment of caspase-3 activity by Western blot and FACS analysis

To assess the levels of caspase-3 (cleaved form) present in cell lysates, equal amounts of total homogenate (40 μg) were diluted in Laemmli sample buffer and boiled at 90 °C for 5 min. Proteins were separated on 15% SDS-PAGE and were transferred to PVDF hybond membrane (Millipore Corporation, Billerica, MA, USA). The membrane was then incubated overnight at 4 °C with (rabbit) anti caspase-3/CPP32 antibody (Biosource International, CA, USA). After washing, the membrane was incubated with a peroxidase-conjugated secondary antibody for 1 h. Immunolabelled bands were then detected using a SuperSignal West Dura (Pierce, Rockford, IL, USA) and quantified using the image analysis Quantity One software (Bio-Rad Laboratories, Milano, Italy). Results were expressed as ratios between the densitometry of the protein of interest and the densitometry of the loading control, β-actin (Santa Cruz Biotechnology Inc., Santa Cruz, CA, USA).

Caspase-3 activity was also quantified by flow cytometry. In brief, single-cell suspensions were incubated with FAM-FLICA™ Caspases 3&7 solution (Caspase 3&7 FLICA kit FAM-DEVD-FMK) for 1 h at 37 °C, washed twice with PBS and analysed using a FACSCanto flow cytometer (Becton-Dickinson, San Jose, CA).

2.13. Mitochondrial membrane potential ($\Delta\psi$)

Mitochondrial membrane potential ($\Delta\psi$) was assessed using tetramethylrhodamine, methyl ester, and perchlorate (TMRM). TMRM is a lipophilic potentiometric dye those partitions between the mitochondria and cytosol in proportion to $\Delta\psi$ by virtue of its positive charge. At low concentrations, the fluorescence intensity is a simple function of dye concentration, which is in turn a direct function of mitochondrial potential. Therefore, the accumulation of dye in mitochondria and the intensity of the signal is a direct function of mitochondrial potential. For confocal microscope analysis, cells were cultured on glass coverslips and loaded with dye by adding the fluorescent probe TMRM, dissolved in 0.1% DMSO (100 nM final concentration), to the cell culture media for 20 min at 37 °C. The cells were fixed in 2.0% buffered paraformaldehyde for 10 min at room temperature and the TMRM fluorescence analysed (at an excitation wavelength of 543 nm) using a confocal Leica TCS SP5 scanning microscope (Mannheim, Germany) equipped with an helium-neon laser source for fluorescence measurements. The observations were performed by collecting the emitted fluorescence with a Leica Plan Apo 63x oil immersion objective. A series of 1.0 μm-thick optical sections (1024 × 1024 pixels) of the cells was taken at intervals of 0.5 μm. A number of optical sections (ranging from 10 to 20) for each examined sample were then projected as a single composite image by superimposition.

Mitochondrial membrane potential was also quantified by flow cytometry. Single-cell suspensions were washed twice with PBS and incubated, in the dark, for 20 min at 37 °C with TMRM (100 nM) in DMEM. After labelling, cells were washed and resuspended in PBS and analysed using a FACSCanto flow cytometer (Becton-Dickinson, San Jose, CA).

2.14. Cell proliferation

Cell proliferation was measured using a fluorometric resazurin reduction method (CellTiter-Blue, Promega Corp.). Resazurin is a redox dye commonly used as an indicator of chemical cytotoxicity in cultured cells [35]. The assay is based on the ability of viable, metabolically active cells to reduce resazurin to resorufin and dihydroresorufin, where the rate of dye reduction is directly proportional to the number of viable cells present. This conversion is intracellular and is facilitated by mitochondrial, microsomal and cytosolic oxidoreductases. The resorufin produced as a result of
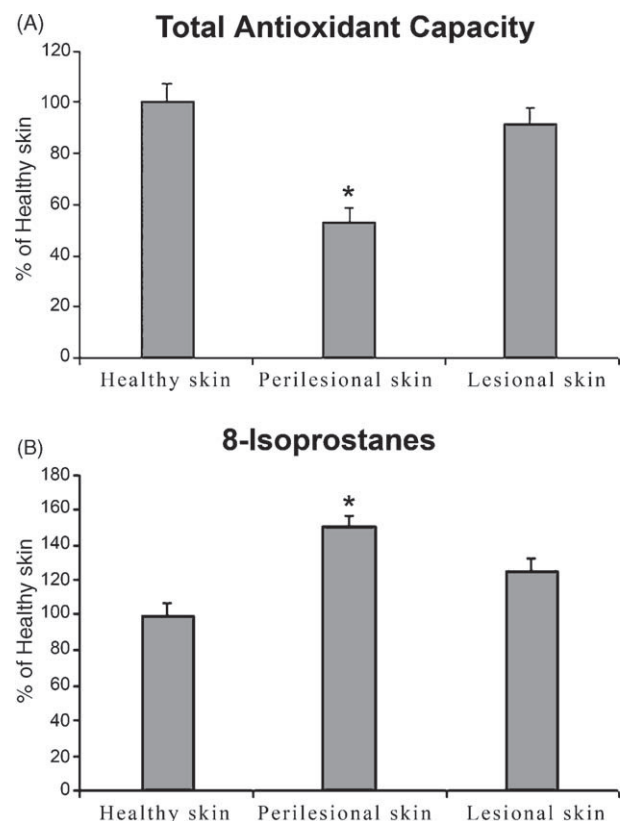
Fig. 3. (A) Cellular TAC. Total antioxidant capacity, expressed in ascorbate equivalent units, was measured by a chemiluminescent assay in the cytosolic fractions of keratinocyte lysates from healthy, perilesional and lesional skin. (B) Rate of lipid peroxidation, quantified according to cytosolic levels of 8-isoprostanes (see Section 2). The reported values (means ± s.d.) are representative of five independent experiments carried out in triplicate. *Significant difference (p ≤ 0.05) vs. keratinocytes from healthy skin.

resazurin bioreduction is measured fluorometrically. Resazurin is non-toxic to cells and stable in culture medium, allowing continuous measurement of cell proliferation in vitro as either a kinetic or endpoint assay.

2.15. Statistical analysis

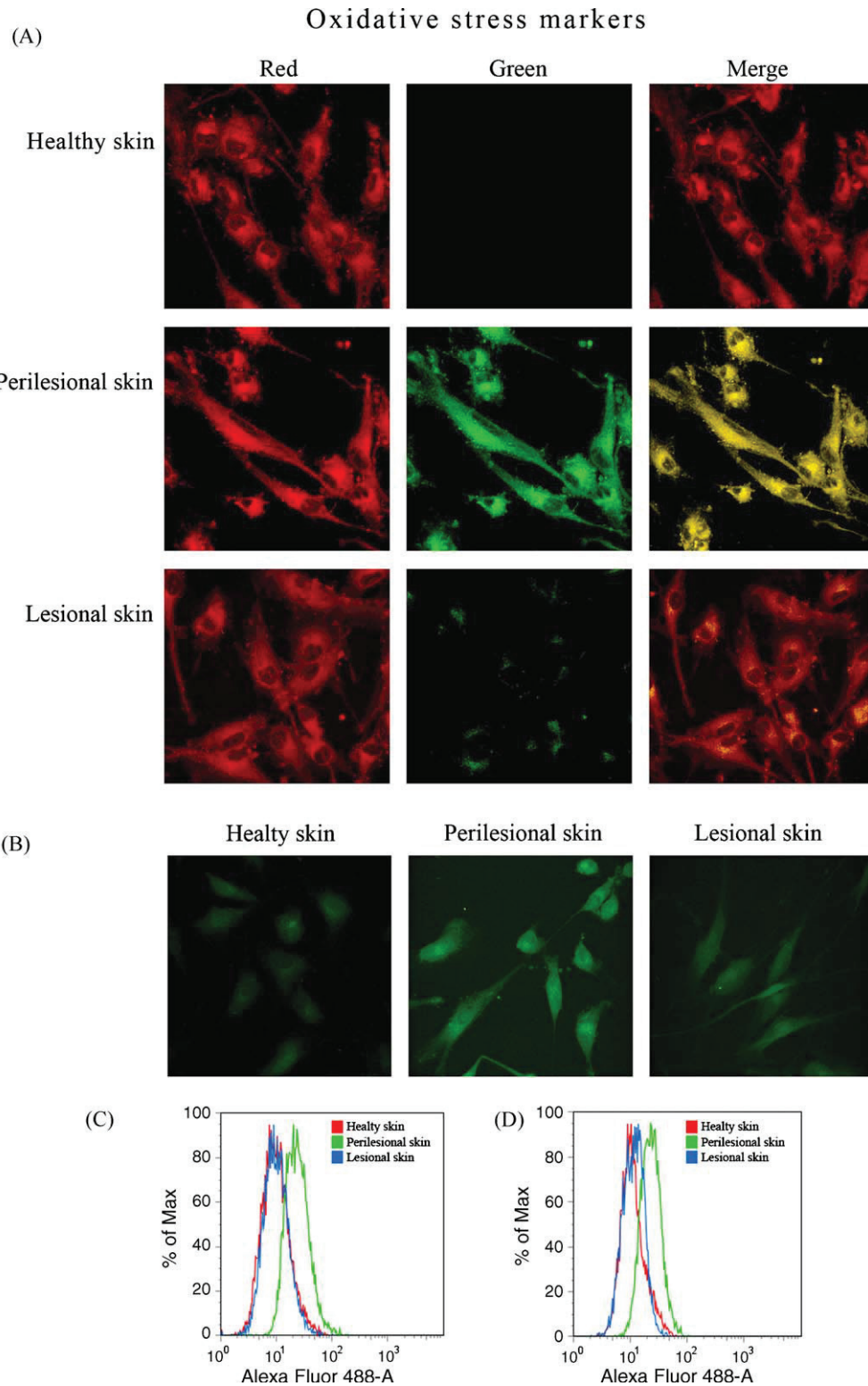All data is expressed as mean ± S.E.M. Comparisons between different groups were performed by ANOVA and then by the

Fig. 4. Oxidative stress markers: (A) Representative confocal microscope images of lipid peroxidation in keratinocytes loaded with the fluorescent probe BODIPY, according to Section 2. (B) Representative confocal microscope images of intracellular ROS production in keratinocytes from healthy, perilesional and lesional skin. Reactive oxygen species formation was also assessed by FACS (D). (C) Flow cytometry analysis of lipid peroxidation. Keratinocytes from healthy, perilesional and lesional skin were loaded with fluorescent probe BODIPY and the green signal detected.
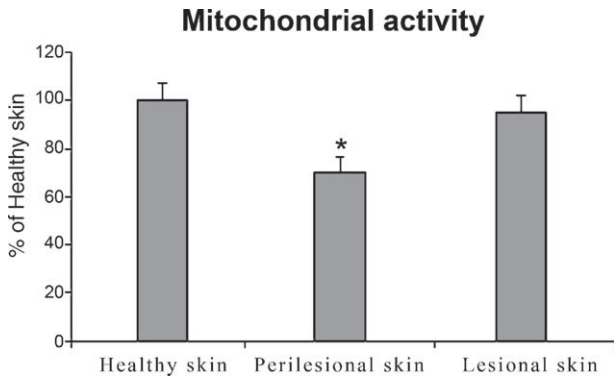
Mitochondrial activity

Fig. 5. Mitochondrial activity in keratinocytes from healthy, perilesional and lesional skin. Mitochondrial activity was checked using the MTT test. Values are expressed as % vs. keratinocytes from healthy skin. The reported values (means ± s.d.) are representative of five independent experiments, each performed in triplicate. *Significant difference ($p \leq 0.05$) vs. keratinocytes from healthy skin.
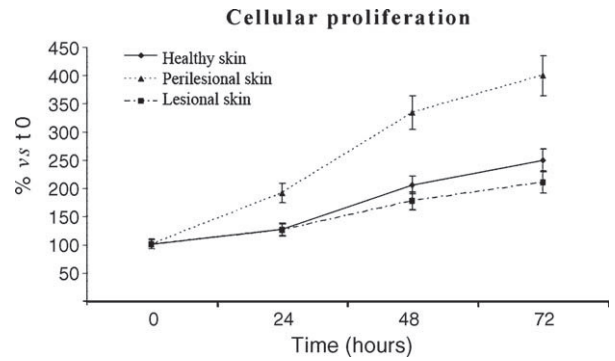
Cellular proliferation

Fig. 6. Cellular proliferation. Cellular proliferation was measured using a fluorometric resazurin reduction method, according to Section 2. The reported values (means ± s.d.) are representative of four independent experiments, each performed in triplicate. *Significant difference ($p \leq 0.05$) vs. keratinocytes from healthy skin.
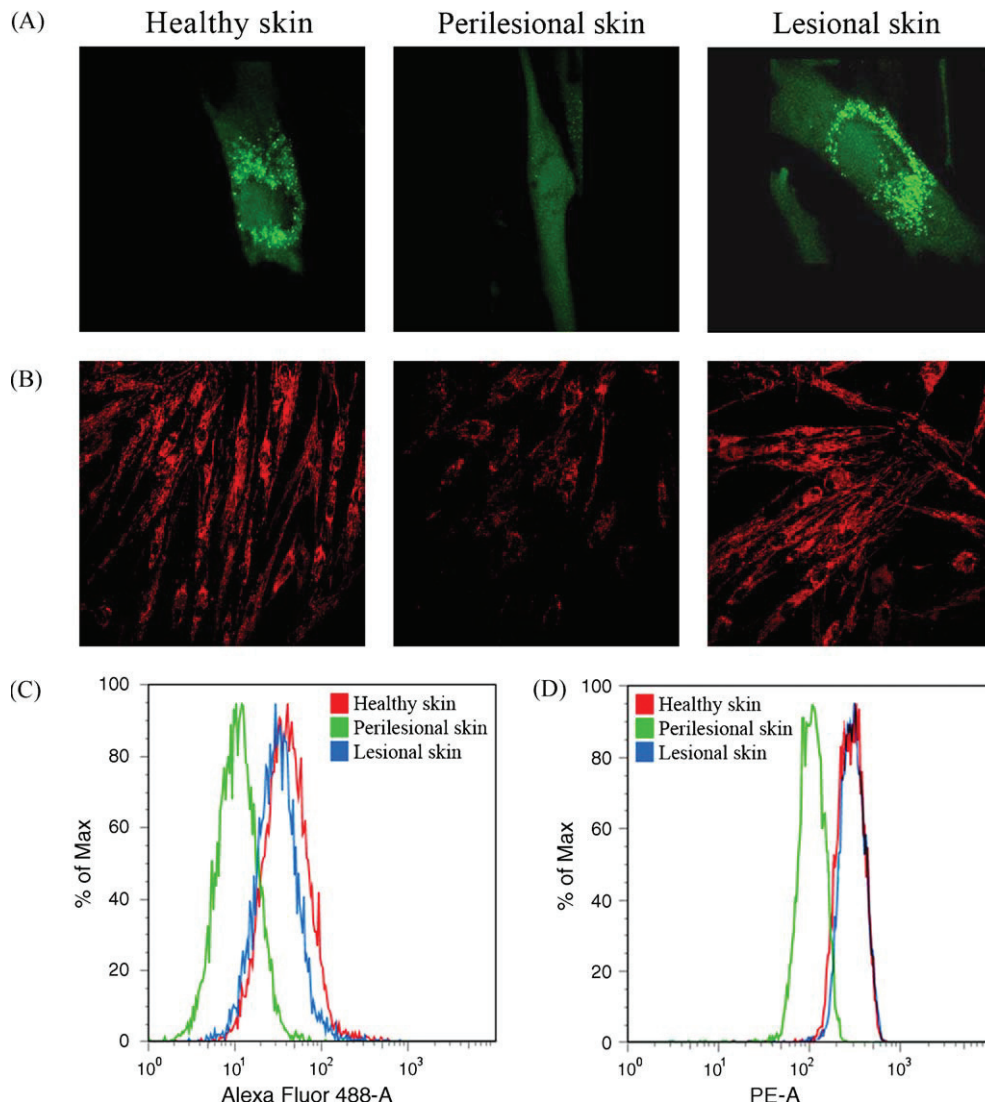

Fig. 7. (A) Representative confocal microscope images showing the mitochondrial permeability transition pore opening in keratinocytes from perilesional skin of vitiligo patients. Mitochondrial fluorescence is evident in keratinocytes from healthy and lesional skin but not in keratinocytes from perilesional skin. Mitochondrial fluorescence was also assessed by FACS analysis (C). (B) Confocal analysis of mitochondrial depolarisation in keratinocytes from perilesional skin. Mitochondrial membrane potential ($\Delta\psi$) was assessed using tetramethylrhodamine, methyl ester, and perchlorate (TMRM). TMRM fluorescence was also detected by FACS analysis (D).

Bonferroni *t*-test. A *p* value of <0.05 was accepted as statistically significant.

3. Results

3.1. Ultrastructural analysis

3.1.1. Lesional skin

The basal membrane appears well preserved but slightly flattened, with anchoring fibrils maintained in the correct position. Melanocytes are not detected in any of the observed fields. Membrane fragments with cytoplasmic density similar to that of the melanocytary cytoplasm are only observed in two patients.

Keratinocytes show no cytoskeletal alterations or substantial reorganisation of intracytoplasmatic organelles, except in those areas characterised by a greater electron density alternated with lighter patches, which are probably vacuoles.

Langerhans cells, located at basal level (Fig. 2), display an indented nucleus, a rough endoplasmic reticulum (RER) and a well-developed Golgi apparatus in the cytoplasm. Typical Birbeck granules (arrow and arrowheads) can be observed inside these cells. The micrograph also shows a remarkable number of larger mitochondria, compared to those present in the Langerhans cells of the normal skin sample from the same patient (asterisk). An additional population of "clear cells", characterised by the presence of an indented nucleus and many RER cisternae, lack Birbeck granules: nevertheless, they are rich in structures, which are present along the concave cisternae of the Golgi apparatus, that have the same electron density as Birbeck granules. These features confer the immunophenotype of immature dendritic cells, or less differentiated Langerhans cells, to these cells.

3.1.2. Perilesional skin

Despite some focal interruptions, the basal membrane appears well developed, with fully organised anchoring fibrils. Melanocytes are well preserved (Fig. 2) and rich in organelles, such as RER, Golgi apparatus and intermediate filaments. Mitochondria appear very large (arrow), reflecting ultrastructural alterations of the cristae.

Most melanocytes show well-preserved melanosomes. These are not detected at the earlier phase of differentiation; on the contrary, melanosomes at the second, third and fourth phases of differentiation are observed (arrowheads). Some of these melanosomes are round in shape and do not show substantial ultrastructural modifications.

Langerhans cells, which have a tendency to localise in the suprabasal level, are particularly abundant. They have a typical ultrastructure, with Birbeck granules present in most cells, though several cells with a more immature phenotype can be observed.

Keratinocytes (Fig. 2) show partial vacuolisation and the presence of granular cytosolic material. The same material is also present in the extracellular environment between melanocytes and keratinocytes, as well as between keratinocytes. Most of the mitochondria have swollen membranes (arrow) and rearranged cristae (arrowhead), as well as a swollen matrix and perimembrane space (asterisk).

3.1.3. Healthy skin

The basal membrane shows well-preserved anchoring fibrils and appears very well developed, with no signs of degeneration.

Melanocytes appear normal in number and size and are characterised by a large number of melanosomes in all differentiative phases, a structured rough endoplasmic reticulum and large but well-preserved mitochondria. In some melanocytes, focal degenerative signs, such as intracellular edema and vacuoles, can be detected.

Langerhans cells, though lacking dendritic structures, appear normal in number and dimension. These cells show the immunophenotype typical of an intermediate differentiation stage, as they all contain Birbeck granules.

Keratinocytes have the ultrastructural features of healthy cells and only in two cases is there reduced distribution of the cytoskeleton, when signs indicating cellular suffering and/or degeneration are absent.

3.1.4. Biochemical assays

As a first attempt to evaluate the extent of oxidative damage in the cultured cells, isoprostane levels and the fluorescence of the lipophilic probe BODIPY were assessed. Fig. 3B shows that isoprostane levels are significantly increased in keratinocytes from perilesional skin, but not in cells from normal and lesional skin. Similarly, the shift in BODIPY fluorescence is only present in cells from perilesional skin (Fig. 4A and C) as shown by confocal microscopy and FACS analysis.

In accordance with these findings, ROS production has been found to be strongly enhanced in perilesional skin (Fig. 4B and D). There is no significant evidence for the presence of ROS in healthy and lesional skin samples.

Total antioxidant capacity (Fig. 3A), being unvaried in lesional skin compared to healthy skin, is clearly reduced in perilesional skin. The keratinocytes from perilesional skin show a marked reduction in mitochondrial activity with respect to healthy and lesional cells, as determined by the MTT reduction test (Fig. 5).

Cell proliferation rate, which was evaluated by the resazurin reduction method assay, revealed a strong increase in cell number in perilesional skin (Fig. 6).
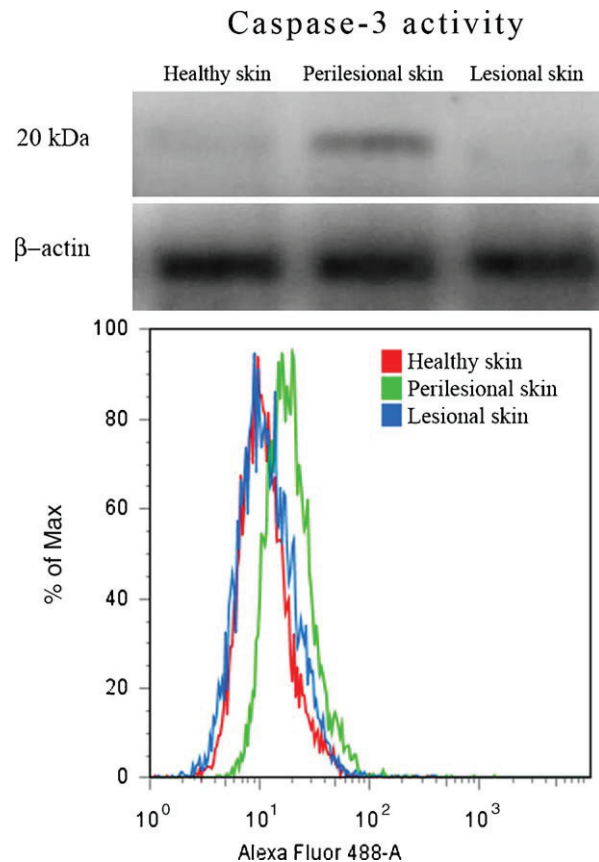

Fig. 8. Western blot analysis of caspase-3 activity. All signals were quantified by densitometric analysis and are expressed as a ratio of NF-kB densitometry of β-actin (loading control) densitometry. Caspase-3 activity was also assessed FACS analysis. Mitochondrial membrane depolarisation in keratinocytes from perilesional skin is accompanied by apoptotic events. No signs of apoptosis are present in healthy and lesional skin.
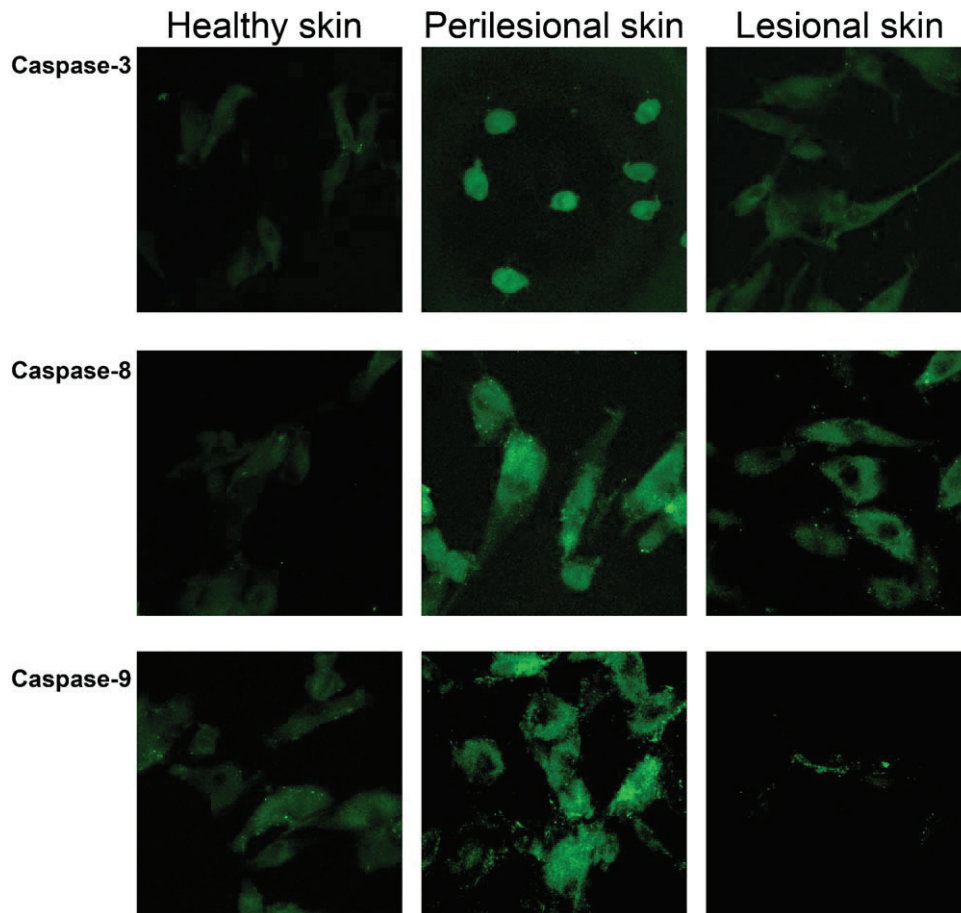
Caspase activation

Fig. 9. Confocal evaluation of caspase activation. The activation of the apoptotic process was assessed by measuring the change in fluorescence in caspase-3, caspase-8 and caspase-9 activity. For details, see Section 2.

Cell viability, which was assessed by the MTT assay, revealed, in perilesional skin, a decrease in mitochondrial activity that was not present in lesional and healthy skin. Confocal and FACS microscopy analysis indicated, in perilesional skin, mitochondrial permeability transition pore opening (Fig. 7A and C) and mitochondrial membrane depolarisation (Fig. 7B and D). These changes were not evident in lesional and healthy skin.

Caspase-3 activity, which was assessed by Western blotting and FACS analysis, indicated that mitochondrial membrane depolarisation in keratinocytes from perilesional skin is accompanied by apoptotic events (Fig. 8). No signs of apoptosis are present in healthy and lesional skin.

Data concerning the apoptotic markers show that caspase-3, caspase-8 and caspase-9 activities were nearly absent in healthy skin, while they were strongly enhanced in perilesional skin (Fig. 9).

4. Discussion

An interesting finding arising from this work is the morphological alterations of mitochondria in keratinocytes from perilesional skin and the increased number of Langerhans cells, in varying differentiative phases, in lesional skin. In keratinocytes, mitochondria appear swollen and lack a normal and organised ultrastructure of internal and external membrane systems; remarkably, they show a relevant subversion of the mitochondrial cristae. Mitochondrial activity plays a crucial role in normal cell function. Indeed, the mitochondrial respiratory chain and oxidative phosphorylation generate energy, in the form of ATP molecules that are needed for the cell's main activities, such as cell differentiation, proliferation and mitosis. Several studies have focussed their attention on the changes in mitochondrial membrane potential, particularly for its possible involvement in the induction of apoptotic mechanisms. One theory is that a collapse in the mitochondrial transmembrane electrical potential would represent an early event and possible cause of programmed cell death [37].

In our study, the mitochondrial alterations observed in perilesional keratinocytes appear to be very similar to those described by Sun et al. in the same cell types during apoptosis [38]. In order to explain the origin of these alterations and to detect additional signs of apoptosis in keratinocytes, we performed a number of biochemical assays in the cultured cells. The results of these measurements show that the ultrastructural alterations found in keratinocytes from perilesional skin are directly related to an impaired mitochondrial activity, with evidence of membrane depolarisation. The mitochondrial damage is associated with an increase in ROS production and, hence, oxidative stress, which is confirmed by the presence of lipoperoxidation markers (BODIPY fluorescence shift and isoprostane levels) and by the concomitant decrease in total antioxidant capacity. At a perilesional level, a marked activation of caspase-3, caspase-8 and caspase-9 – three strong indicators of the apoptotic process – was also observed. In light of previous studies [10,39–41], which report a role for

F. Prignano et al. / Journal of Dermatological Science 54 (2009) 157–167

oxidative stress in lesional vitiligo skin, our data suggest a possible involvement of perilesional keratinocytes in (the impairment of) damaging the epidermis, as a result of increased oxidative stress and a reduction in antioxidant levels.

According to the current view of the apoptotic pathway, it is accepted that initial cell stress, caused by an overproduction of free radicals in the epidermis, activates the pro-apoptotic members of the bcl-2 family. These proteins are localised in the cytosol, where they act as probes for cell damage or stress; once activated, they relocate to the mitochondrial surface, thereby leading to the formation of transmembrane pores (Permeability Transition Pore, or PT pore). These pores, which are responsible for mitochondrial membrane depolarisation and for the reduction of mitochondrial activity, promote the release of many pro-apoptotic proteins, such as cytochrome c and various molecules from the intermembrane space [42]. Once released into the cytosol, these proteins promote the activation of caspase-9, the initiator caspase [43,44], which can in turn activate the effector caspases, such as caspase-3 and caspase-6. The latter are responsible for the cleavage of key cellular proteins, such as cytoskeletal proteins, leading to the typical morphological changes observed in cells undergoing apoptosis [45].

Our results also clearly indicate an increase in caspase-8 activity. This finding is in agreement with a recent report [46] describing significantly higher levels of TNF-alpha and FasL in the depigmented epidermis, which indicates a role for these factors in increasing apoptosis. In this study, PTEN (phosphatase and tension homologue), which could inhibit the phosphatidylinositol 3-kinase/protein kinase B (PI3K/Akt) signalling pathway was significantly higher in the depigmented epidermis, implying that vitiliginous keratinocytes may be more susceptible to TNF-alpha-mediated apoptosis through impaired Akt and NF-kB activation.

As reported by Lee et al., apoptotic keratinocytes appear to cause a decrease in SCF (Stem Cell Factor) synthesis. In these in vitro studies, apoptotic keratinocytes produce lower levels of SCF mRNA and SCF proteins compared to normal keratinocytes. SCF plays an important role in melanocyte survival and proliferation, as indicated by the induction of apoptosis in melanocytes when SCF is removed. These results could also apply to in vivo findings. Furthermore, keratinocyte apoptosis induces a decrease in the synthesis of other melanocyte growth factors, such as bFGF, where a loss of these melanocyte survival factors causes melanocyte apoptosis, resulting in their disappearance from the lesions of vitiligo patients [47–50].

Our study highlights, for the first time, that the biochemical and ultrastructural alterations were primarily observed in perilesional skin, rather than in lesional or healthy skin. This leads us to suggest that perilesional skin represents the substrate where melanocyte death is initiated. The extent to which these cells are destroyed depends on the evolution of the disease and on the "noxa", which stimulates the damage. It is possible that the alteration of mitochondrial functionality and, perhaps, an apoptotic induction is responsible for the observed melanocytic damage. The endpoint of this biological event might cause the death of melanocytes in lesional skin, with an increase in Langerhans cells possibly due either to a subversion of the normal epidermic reorganisation or, more likely, a stimulation by local biohumoral factors (as proved by the increased number of Langerhans cells displaying an immature phenotype).

Besides considering the achromic patch as the terminal event of a chain of biological processes that take place in perilesional skin, our data suggests that keratinocytes play a very important role in vitiligo development. Keratinocytes should no longer be considered as innocent bystanders of immunological events but as real, integrative components of the melanic unit formed by melanocytes, keratinocytes and Langerhans cells in the epidermis.

References

[1] Huggins RH, Schwartz RA, Krysicka Janniger C. Vitiligo. Acta Dermatoven APA 2005;14:4.
[2] Taieb A, Picardo M. The definition and assessment of vitiligo: a consensus report of the vitiligo European Task Force. Pigment Cell Res 2007;20:27–35.
[3] Barnes L, Nordlund JJ. Vitiligo. In: Dermis J, editor. Clinical dermatology. Philadelphia: Lippincott; 1995. p. 11–33.
[4] Kovacs SO. Vitiligo. J Am Acad Dermatol 1998;38:647–66.
[5] Ortonne JP, Bose SK. Vitiligo: where do we stand? Pigment Cell Res 1993;6:61–72.
[6] Mollet I, Ongenae K, Naeyaert JM. Origin, clinical presentation and diagnosis of hypomelanotic skin disorders. Dermatol Clin 2007;25:363–71.
[7] Rezaei N, Gavalas NG, Weetman AP, Kemp EH. Autoimmunity as an aetiological factor in vitiligo. J Eur Acad Dermatol Venereol 2007;21:865–76.
[8] Ongenae K, Van Geel N, Naeyaert JM. Evidence for an autoimmune pathogenesis of vitiligo. Pigment Cell Res 2003;16:90–100.
[9] Schallreuter KU, Wood JM, Ziegler I, Lemke KR, Pittelkow MR, Lindsey NJ, et al. Defective tetrahydrobiopterin and catecholamine biosynthesis in the depigmentation disorder vitiligo. Biochim Biophys Acta 1994;1226:181–92.
[10] Maresca V, Roccella M, Camera E, Del Porto G, Passi S, Grammatico P, et al. Increased sensitivity to peroxidase agents as a possible pathogenetic factor of melanocyte damage in vitiligo. J Invest Dermatol 1997;109:310–3.
[11] Picardo M, Passi S, Morrone A, Grandinetti M, Di Carlo A, Ippolito F. Antioxidant status in the blood of patients with active vitiligo. Pigment Cell Res 1994;7:110–5.
[12] Koka R, Armuctu F, Altinyazar HC, Gurel A. Oxidant–antioxidant enzymes and lipid peroxidation in generalized vitiligo. Clin Exp Dermatol 2004;29:406–9.
[13] Hann SK. A role of the nervous system in the pathogenesis of segmental vitiligo. Pigment Cell Res 1999;7:26.
[14] Grines PE. White patches and bruised souls: advances in the pathogenesis and treatment of vitiligo. J Am Acad Dermatol 2004;51:85–7.
[15] Schallreuter KU, Wood JM, Ziegler I, Lemke KR, Pittelkow MR, Lindsey NJ, et al. Defective tetrahydrobiopterin and catecholamine biosynthesis in the depigmentation disorder vitiligo. Biochim Biophys Acta 1994;1226:81–92.
[16] Schallreuter KU, Wood JM, Pittelkow MR, Buttner G, Swanson N, Korner C, et al. Increased monoamine oxidase A in the epidermis of patients with vitiligo. Arch Dermatol Res 1996;288:14–8.
[17] Yu. Melanocyte destruction and repigmentation in vitiligo: a model for nerve cell damage and regrowth. J Biomed Sci 2002;9:564–73.
[18] Al'Abadie MSK, Warren MA, Bleehen SS. Morphologic observations on the dermal nerves in vitiligo: an ultrastructural study. Int J Dermatol 1995;34:837–40.
[19] Halaban R, Langdom R, Birchall N, Cuono C, Baird A, Scott G, et al. Basic fibroblastic growth factor from human keratinocytes is a natural mitogen for melanocytes. J Cell Biol 1988;107:1611–9.
[20] Swope VB, Abdel-Malek Z, Kassem LM, Nordlund JJ. Interleukins 1 alpha and 6 and tumor necrosis factor alpha are paracrine inhibitors of human melanocyte proliferation and melanogenesis. J Invest Dermatol 1991;96:180–5.
[21] Imokaua G, Yada Y, Rimura M, Morisaki N. Granulocyte/macrophage colony-stimulating-factor IA an intrinsic keratinocyte-derived growth factor for human melanocytes in UVA-induced melanosis. Biochem J 1996;313:625–31.
[22] Grichnik JM, Burch JA, Burchette J, Shea CR. The SCF/KIT pathway plays a critical role in the control of normal human melanocyte homeostasis. J Invest Dermatol 1998;11:233–8.
[23] Imokawa G. Autocrine and paracrine regulation of melanocytes in human skin and in pigmentary disorders. Pigment Cell Res 2004;17:96–110.
[24] Fitzpatrick TB, Breathnach AS. Die epidermale Melanin-Einheit-system. Dermatol Woechenschr 1963;147:635–42.
[25] Hautmann G, Moretti S, Lotti T, Hercogovà J. Pathogenesis of Vitiligo: evidence for a possible ongoing disorder of the cutaneous microenvironment. In: Lotti T, Hercogova J, editors. Vitiligo: new data and hypotheses. New York, Basel: Marcel-Dekker; 2004. p. 99–121.
[26] Moretti S, Spallanzani A, Amato L, Hautmann G, Gallerani I, Fabbri P. Vitiligo and epidermal microenvironment: possible involvement of keratinocyte-derived-cytokines. Arch Dermatol 2002;138:273–4.
[27] Dell'Anna ML, Picardo M. A review and a new hypothesis from non-immunological pathogenetic mechanisms in vitiligo. Pigment Cell Res 2006;19:406–11.
[28] Bhawan J, Butani K. Keratinocyte damage in vitiligo. J Cutan Pathol 1983;10:207–12.
[29] Hann SK, Park YK, Lee KG, Choi EH, Im S. Epidermal changes in active vitiligo. J Dermatol 1992;19:217–22.
[30] Galadri E, Mehregan AH, Hashimoto K. Ultrastructural study of vitiligo. Int J Dermatol 1993;32:269–71.
[31] Montes LF, Abulafia J, Wilborn WH, Hyde BM, Montes CM. Value of histopathology in vitiligo. Int J Dermatol 2003;42:57–61.

[32] Panuncio AL, Vignale R. Ultrastructural studies in stable vitiligo. Am J dermatopathol 2003;25:16–20.

[33] Bradford MM. A rapid and sensitive method for the quantitation of microgram quantities of protein utilizing the principle of protein–dye binding. Anal Biochem 1976;72:248–54.

[34] Drummen GPC, Gadella BM, Post JA, Brouwers JF. Mass spectrometric characterization of the oxidation of the fluorescent lipid peroxidation reporter molecule C11-BODIPY581/591. Free Rad Biol Med 2004;36:1635–44.

[35] Zhang HX, Du GH, Zhang JT. Assay of mitochondrial functions by resazurin in vitro. Acta Pharmacol Sin 2004;25:385–9.

[36] Petronilli V, Miotto G, Canton M, Brini M, Colonna R, Bernardi P, et al. Transient and longlasting openings of the mitochondrial permeability transition pore can be monitored directly in intact cells by changes in mitochondrial calcein fluorescence. Biophys J 1999;765:725–54.

[37] Zamzami N, Marchetti P, Castedo M, Decaudin D, Macho A, Hirsch T, et al. Sequential reduction of mitochondrial transmembrane potential and generation of reactive oxygen species in early programmed cell death. J Exp Med 1995;182:367–77.

[38] Sun MG, Williams J, Munoz-Pinedo C, Perkins GA, Brown JM, Ellisman MH, et al. Correlated three-dimensional light and electron microscopy reveals transformation of mitochondria during apoptosis. Nat Cell Biol 2007;9:1057–65.

[39] Schallreuter KU, Moore J, Wood JM, Beazley WD, Gaze DC, Tobin DJ, et al. In vivo and in vitro evidence for hydrogen peroxide (H_2O_2) accumulation in the epidermis of patients with vitiligo and its successful removal by a UVB-activated pseudocatalase. J Invest Dermatol Symp Proc 1999;4:91–6.

[40] Passi S, Grandinetti M, Maggio M, Stancato A, De Luca C. Epidermal oxidative stress in vitiligo. Pigment Cell Res 1998;11:81–5.

[41] Schallreuter KU, Wood JM, Berger J. Low catalase levels in the epidermis of patients with vitiligo. J Invest Dermatol 1991;97:1081–5.

[42] Webb SJ, Harrison DJ, Wyllie AH. Apoptosis. An overview of the process and its relevance in disease. Adv Pharmacol 1997;41:1.

[43] Joza N, Susin SA, Daugas E, Stanford WL, Cho SK, Li CY, et al. Essential role of the mitochondrial apoptosis-inducing factor in programmed cell death. Nature 2001;410:549–54.

[44] Shi Y. A structural view of mitochondria-mediated apoptosis. Nat Struct Biol 2001;8:394–401.

[45] Salvesen GS, Riedl SJ. Caspase mechanisms. Adv Exp Med Biol 2008;615:13–23.

[46] Kim NH, Jeon S, Lee HJ, Lee AY. Impaired PI3K/Akt activation-mediated NF-kappaB inactivation under elevated TNF-alpha is more vulnerable to apoptosis in vitiliginous keratinocytes. J Invest Dermatol 2007;127:2612–7.

[47] Lee AY, Youm YH, Kim NH, Yang H, Choi WI. Keratinocytes in the depigmented epidermis of vitiligo are more vulnerable to trauma (suction) than keratinocytes in the normally pigmented epidermis, resulting in their apoptosis. Br J Dermatol 2004;151:995–1003.

[48] Lee AY, Kim NH, Coi WI, Youm YH. Less keratinocyte-derived factors related to more keratinocyte apoptosis in depigmented than in normally pigmented suction-blistered epidermis may cause passive melanocyte death in vitiligo. J Invest Dermatol 2005;124:976–83.

[49] Bondanza S, Maurelli R, Paterna P, Migliore E, Di Giacomo F, Primavera G, et al. Keratinocyte cultures from involved skin in vitiligo patients show an impaired in vitro behaviour. Pigment Cell Res 2007;20:288–300.

[50] Huang CL, Nordlund JJ, Boissy R. Vitiligo a manifestation of apoptosis? Am J Dermatol 2002;3:301–8.